*Int. J. Electrochem. Sci.*, 12 **(2017)** 2441 – 2452, doi: 10.20964/2017.03.43

International Journal of
ELECTROCHEMICAL
SCIENCE
www.electrochemsci.org

# Controllable Synthesis of Fusiform-shaped Te@Au hybrids for Efficient Electrocatalytic Oxidation of Isopropanol

*Huile Jin*[1,2], *Liyun Chen*[1], *Aili Liu*[1,2], *Dewu Yin*[2], *Guodong Yu*[2], *Shun Wang*[2,*], *Weizhong Jiang*[1,*]

[1] College of Materials Science and Engineering, Donghua University, Shanghai, P. R. of China 201620;
[2] Nano-materials & Chemistry Key Laboratory, Wenzhou University, Wenzhou, Zhejiang, China 325035
[*]E-mail: shunwang@wzu.edu.cn, jwzh@dhu.edu.cn

*Received:* 28 November 2016 / *Accepted:* 15 January 2017 / *Published:* 12 February 2017

In this study, Te@Au hybrids with the shape of fusiform were successfully prepared through a simple two-phase interfacial reaction and were subsequently applied as the electrocatalysts for the oxidation of isopropanol. Comparing with poly-Au, the Te@Au hybrids showed excellent performance in the oxidation of isopropanol, such as higher limiting current density, better stability, etc. Characterization with electron scanning microscopy reveals that there are numerous edges and defects on the Te@Au surface. The presence of a large number of defects/edges on the catalyst surface, together with the intimate connection between Te and Au, is suggested to be responsible for the observed high electrocatalytic performance. This study presents a new direction for developing low-cost, highly efficient electrocatalysts of direct alcohol fuel cell.

**Keywords:** Te@Au hybrids; Isopropanol; electrocatalytic oxidation; Direct alcohol fuel cell

## 1. INTRODUCTION

Alcohol oxidation reaction (AOR) plays an important role in direct alcohol fuel cells. Precious metals such as Pt exhibited most efficient catalytic activity for the AOR[1,2]. However, the high price and poor durability remain to be the two of drawbacks that preclude the large-scale commercial application of Pt-based catalysts[3]. To overcome these problems, recent efforts have been dedicated to develop novel structured catalysts for improving their electrocatalytic activity and therefore reducing the amounts of catalysts required for the AOR[4,5]. Promising results have been reported on Pt-based binary and ternary alloys[6], carbon supported Pt[7], transition metal alloys[8], oxides[9], or

carbides[10] and hetero-structured Au[11]. Among them, hetero-structured Au nanomaterials is one of the promising catalysts for AOR.

A wide range of hetero-structured Au nanomaterials, including Au/Pd, Au/Pt, PdAu/C, Au/C and Au/Ni-fiber have recently been demonstrated to show AOR activities which are comparable to Pt catalysts[12-16]. Of particular interest, Zhou and co-workers have reported that $Au/SiO_2$ with a cavity structure exhibited excellent electrocatalytic activity for AOR[17]. Cui and co-workers have also demonstrated that $Au/TiO_2$ hetero-nanostructure had a highly efficient activity, stability, and anti-poisoning ability in the eletro-oxidation of ethanol[18]. More recently, depositing Au on the $CeO_2$ or Te semiconductors has also been proved to have synergetic effects on their AOR eletrocatalytic activity[19,20].

A number of investigations have indeed illustrated the existence of so-called synergistic effects when Au are deposited on a semiconductor surface[21-23]. In this work, Te@Au hybrids catalysts were fabricated by using Te crystals as a template and the reducing agent. Different from the approach developed earlier for the fabrication of Au composites, the current method only requires the prefabrication of Te crystals with a desired morphology. More attractively, the template/reducing agent approach has an inherent advantage in implementing a growth limit on the thickness of the shell layer, which consequently reduces the need of the precious metal Au. The fact that the thus-prepared film is thin may in turn improve the synergistic interaction of Au layer and the semiconductor substrates.

The as-prepared Te@Au was subsequently investigated as the potential electrocatalysts of small alcohols. The first four aliphatic alcohols (such as methanol, ethanol, propanol, and butanol) have been recognized as promising fuels because they have easy access, availability and storages which allow them to be used in fuel cells, and equally important, they can be synthesized chemically or biologically[24-27]. Butanol and propanol are considerably less volatile and less toxic than methanol[28-30]. As the smallest secondary alcohol molecule, isopropanol is of great importance in the fundamental studies of fuel cells[31,32], because of its higher chemical performance and faster electron oxidation kinetics[33]. The results reported in the following complement those recent reports on the use of Au to prompt the electrooxidation of simple alcohols[34-40].

## 2. EXPERIMENTAL

### *2.1. The preparation of Te and Te@Au composites*

Potassium hydroxide, ethylene glycol, $HAuCl_4 \cdot 4H_2O$, hydrazine (50%), acetone, and isopropanol used as received from Shanghai Chemical Factory, China. Hexadecyltrimethylammonium bromide (CTAB), Nafion (5 wt% in ethanol), and 2,2'-Dithiodibenzoic Acid (DTBA) were obtained from Aldrich. Tellurium IV diethyldithiocarbamate (TDEC) was purchased from Lianlian Chemical Group, China. Deionized water was fabricated with a Millipore system and was used throughout this study. Te crystals were prepared by dissolving 0.1 g TDEC (0.13 mmol) and 1.0 g CTAB (2.74 mmol) in 27.6 mL $CHCl_3$ solution in an autoclave, followed by adding 0.2 g DTBA (0.65 mmol). The autoclave was placed in an oven to react for 3 hours at a temperature of 130℃. The thus obtained solid

was collected by centrifugation of the reaction solution, followed with washing with deionized water and ethanol three times. Finally the solid was dried in a vacuum at 60℃ for 5 hours.

The preparation of Te@Au hybrids were synthesized as described in the following: Te samples (0.146mmol) was added into ethylene glycol (20.0 mL), followed by the addition of 10 mM $HAuCl_4$ solution (4 mL). The mixture was stirred at 50℃ for 2 hours, which ensured that the Au precursor had been reduced completely. The Te@Au hybrids were collected by centrifuge, followed by washing with water and anhydrous ethanol three times. Finally, the product was dried in a vacuum at 60℃ condition for several hours.

### *2.2. The construction of working electrodes*

To prepare the working electrodes, a glassy carbon (GC) electrode was polished with 50μm alumina powder. After rinsing with deionized water, the cleaned GC electrodes were sonicated in acetone and then in deionized water respectively for a few minutes. Then the above cleaned glassy carbon electrode was driedwith nitrogen. To prepare the coating ink, about 10 mg of Te@Au composites were blended in 4.0 mL of ethanol and 100.0 uL of Nafion solution and the mixture was ultrasonicated for about 30 min. The catalyst ink (20 μL) was then spread on the surface of a glassy carbon electrode (0.124 $cm^2$). A polycrystalline Au electrode purchased from Chenhua Co. China, was investigated for comparison. An Au electrode with a diameter of 1.5 mm, was first polished with 0.1 mm alumina power for nearly 5 min, followed by rinsing the electrode with deionized water. Electrochemical pretreatment of the working electrode was performed in a 0.5 M $H_2SO_4$ solution for 10min with the cyclic voltammetry tests. The scan rate was 100 mV $s^{-1}$ and the scan range was from -0.2 V to 1.1 V (vs. Ag/AgCl).

### *2.3. Characterization of the catalysts and electrochemical measurements*

The Te and Te@Au products were characterized by SEM (FEI Nova Nanosem 200 scanning electron microscope), TEM (JEOL 2100F microscope with a 200 kV), XRD(Bruker D8 Advance diffractometer using Cu Ka radiation with a Ni-filter). Electrochemical tests such as cyclic voltammetry (CV) tests were measured on a CHI660D electrochemical analyzer using a standard three-electrode electrochemical system, with the Te@Au modified GC serving as a working electrode, Ag/AgCl (saturated KCl) as a reference electrode, and a Pt wire as the counter electrode. The stability of the catalyst was evaluated using chronoamperometry in a 0.5 M KOH solution at an applied potential of 0.2 V (vs. Ag/AgCl).

## 3. RESULTS AND DISCUSSION

Fig. 1 shows a SEM image of the Te crystals synthesized at different conditions: panels (a1) and (b1): 0.1g TDEC+1.0g CTAB; (a2) and (b2): 0.2g TDEC+0.6g CTAB, and (a3) and (b3): 0.2g TDEC+0.5g CTAB. Other conditions are 0.2g DTBA and 27.6 ml $CHCl_3$. The magnified SEM images in the (b) panels illustrate that as the reactant concentrations were adjusted, 3D Te crystals of different

shapes were readily obtained, in which the crystal in (b1) looks like a fusiform while Te products in (b2) and (b3) are butter-fly shaped. It can be seen from the magnified SEM image that these Te crystals have a length of up to 30 mm. Those secondary planes have rough edges, providing potential active sites for catalytic reactions.

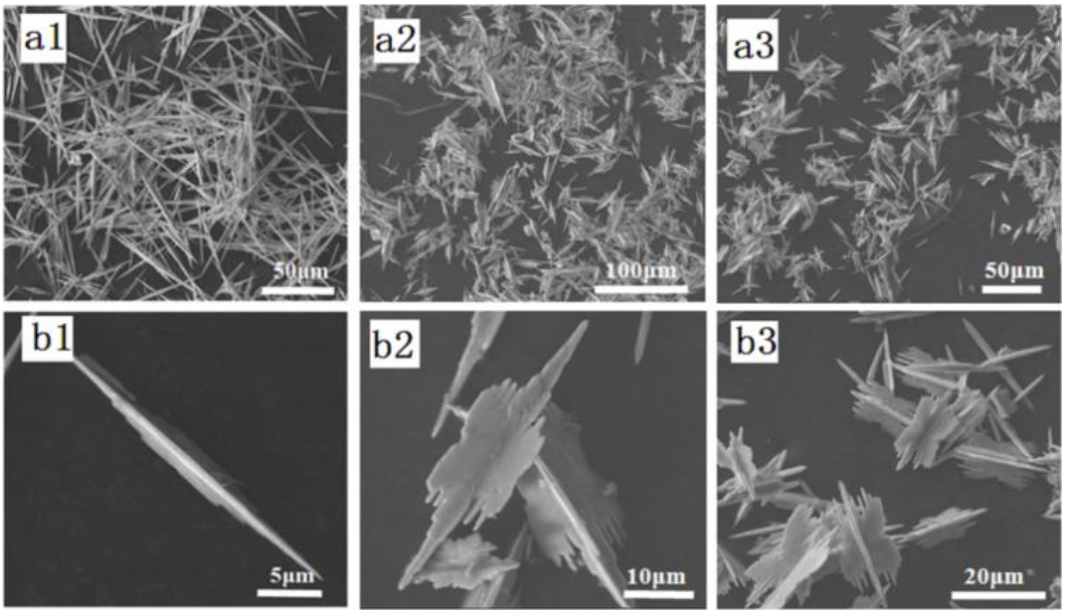


**Figure 1.** SEM images of the Te crystals synthesized at different conditions: panels (a1) and (b1): 0.1g TDEC+1.0g CTAB; (a2) and (b2) 0.2g TDEC+0.6g CTAB, and (a3) and (b3) 0.2g TDEC+0.5g CTAB. Other conditions are 0.2g DTBA and 27.6 ml $CHCl_3$.

Fig. 2 shows (a) XRD and (b) EDS spectra of the Te crystal. In the XRD spectrum the prepared Te could be fitted to the the hexagonal Te according to the literature values (JCPDS card no. 89-4899). These sharp and strong diffraction peaks implied that the Te was well-crystallized. The Te product was a high purity sample because of no impurity peaks in the spectrum. EDS spectrum also confirmed that the products were made up of pure Te elements.

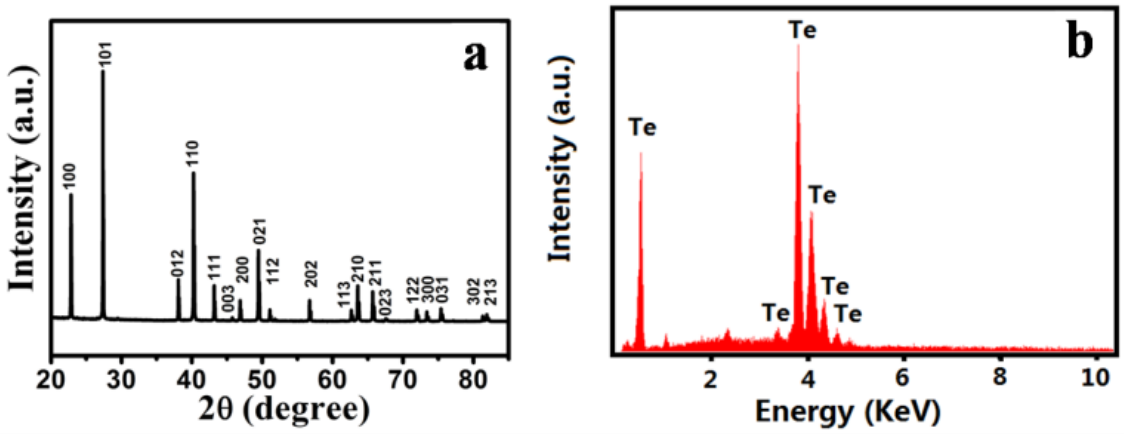


**Figure 2.** (a) XRD and (b) EDS patterns of the Te Nanoneedle shown in Figure 1a.

To understand how the fusiform (see Fig.1 (b1)) and butterfly (Fig. 1(b2)) shaped Te crystals are developed, SEM images of Te products collected at different reaction times were analyzed. Those images in Fig. 3 indicates that after 1.5 hours reaction time, the Te products are mainly made up by micro/nano-sized particles, while only a small portion of them look rhombus-shaped, setting up the stage for the subsequent development of fusiform. After 2 hours, most of them have evolved into fusiforms with sharp ends and have a length between 8～10μm, As seen in Fig. 3c, after 2.5 hours reaction time, the products became dominated by fusiforms, although their length varies. When the reaction time was extended to 3 hours, fusiform shaped Te crystals were fully developed. From the XRD analysis, the growth can be attributed to the preference growth of Te along its (003) facet. As the concentration of the Te precursor (i.e., TDEC) was increased, the sides of Te fusiform grew into a large plane, forming butterfly shape.

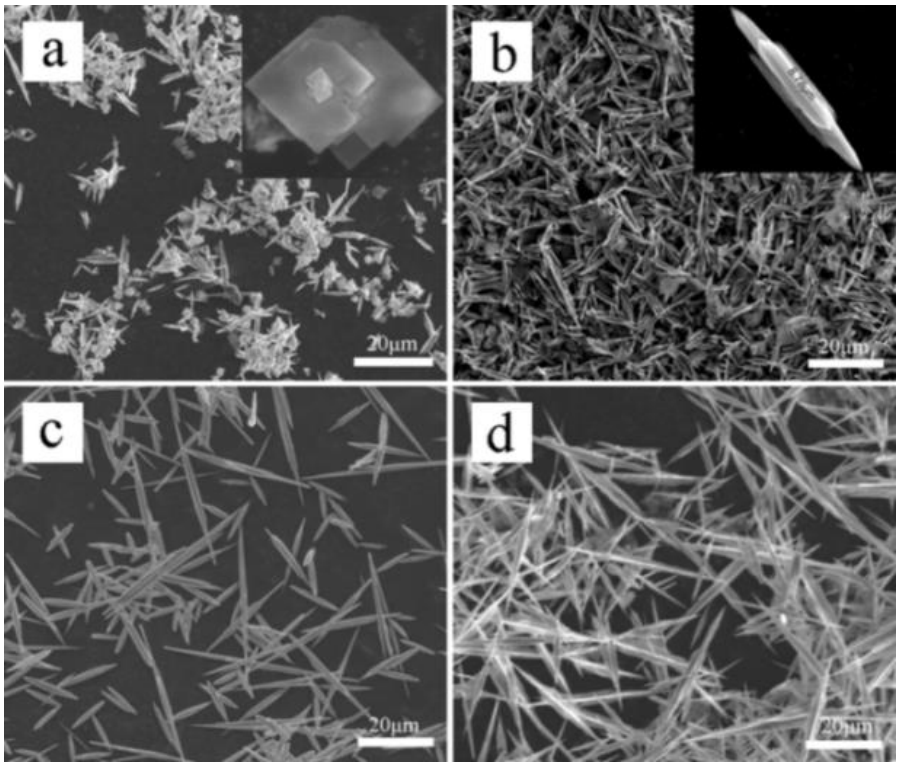


**Figure 3.** SEM images of Te products collected at different reaction times: (a) 1.5h, (b) 2h, (c) 2.5h, (d) 3h

Fig. 4 shows SEM images of (a) Te@Au hybrids which suggests that the fusiform framework was not destroyed during the reduction reaction between Te and $Au^{3+}$ ions. HAADF-STEM taken at the area circled in Fig. 4(b) illustrates the formation of a thin layer of Au film on the Te crystal. For the Te@Au hybrids, five peaks assigning to the (111), (200), (220), (311) and (222) crystalline planes of a face-centered cubic structure of Au have been observed (JCPDS No. 04-0784). This result suggests that Te has been well-covered by Au coating. EDS spectrum in Fig. 4(d) further confirms that Au has successfully deposited on Te.

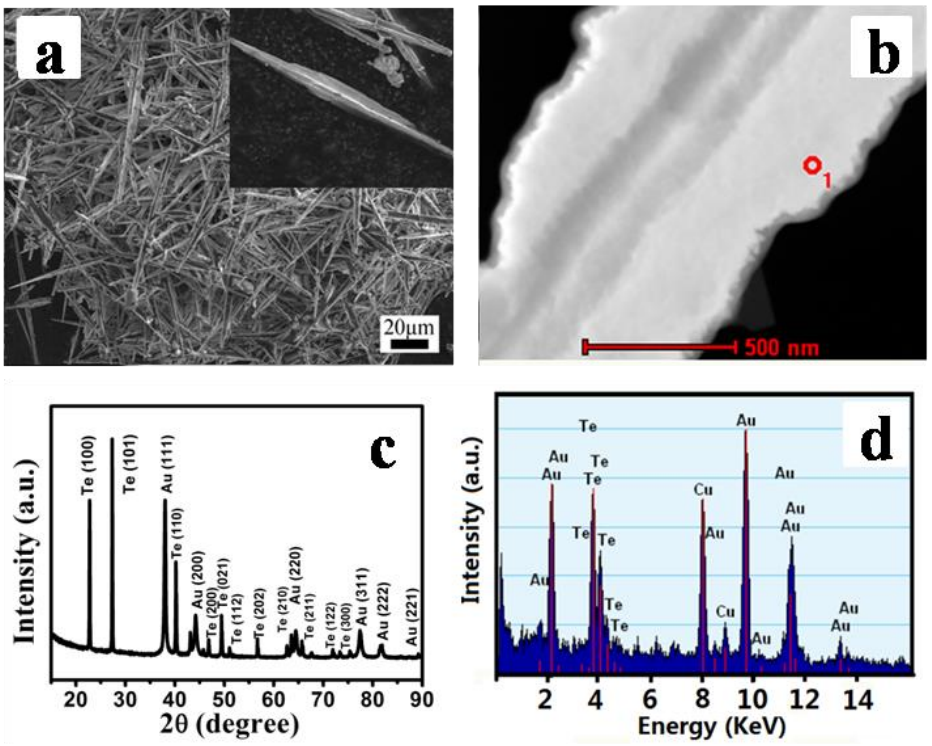


**Figure 4.** SEM images of (a) Te@Au hybrids (b) HAADF-STEM image of the Te@Au hybrids, (c) XRD and (d) EDS patterns of Te@Au hybrids.

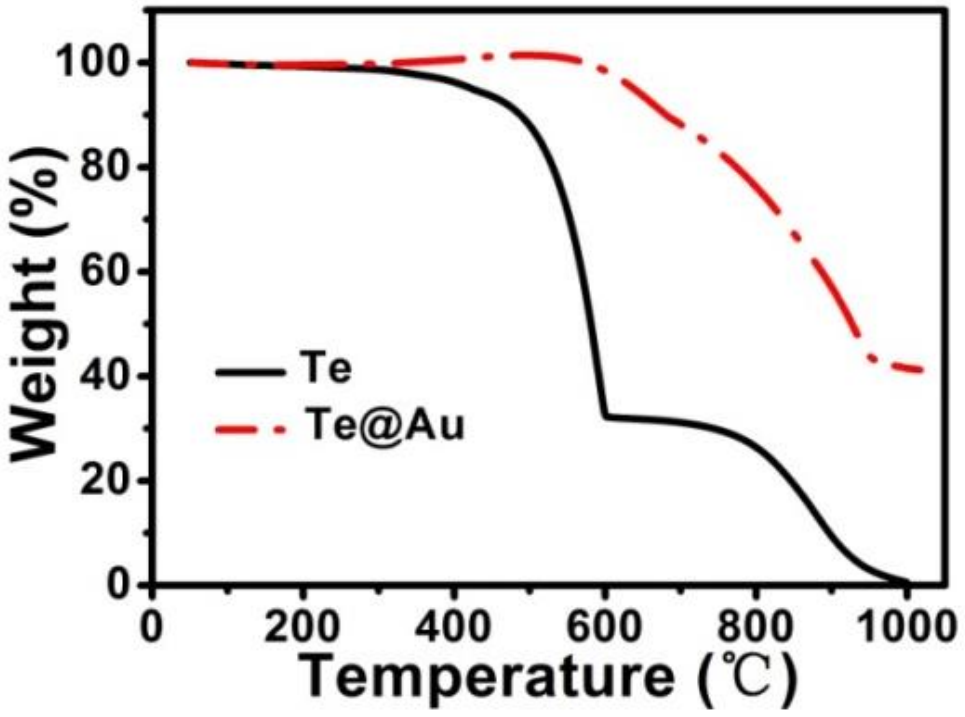


**Figure 5.** TG curves of Te@Au hybrids (red), and Te products (black). The heating rate was 10℃ $min^{-1}$ under nitrogen flow.

Thermogravimetry (TG) method analyzed the average Au content in those Te@Au hybrids.The heating rate was 10 °C $min^{-1}$ under nitrogen flow.TG curves of Te and Te@Au hybridswere shown in Fig.5. From this figure, the Te exhibited a two-step weight-loss process, in which the first weight loss occurred under 400°C.In the TG curve, there was nearly no mass loss, this indicated that the process was dominated with the melting of tellurium crystal. The second weight-lossprocess was attributed to the vaporization of Te. Notably, when the temperature was increased to 1000 °C, Te had completely disappeared. Therefore, Au content in the Te@Au hybrids can be calculated through recording the mass at 1000 °C. As shown in Fig. 5 the calculated Aucontents were 41.5% for the Te@Au hybrids examined here.

CVs of the polycrystalline Au and Te@Au composites catalysts were conducted in a 0.5 M KOH solution and the results are presented in Fig. 6. The poly-Au electrode shows a broad oxidation peak in the potential range between 0.1 and 0.4 V and a characteristic reduction peak at 0.1 V. This is a typical behavior of Au in KOH solution, where the observed electrochemical activities correspond respectively to the formation and removal of the oxides respectively. With the electrode that was prepared with Te@Au composites, the CV resembles that of poly-Au electrode, but with a stronger peak current. The increased peak current may be attributed to the significant increase of the surface area. According to literature, the effective surface area (ESA) of both working electrodes can be estimated from the amount of charge consumed during the reduction of the surface Au oxide monolayer divided by a reported parameter value of 386 mC $cm^{-2}$. The significant increase in ESA arises from the 3D structure of Te crystal and suggests that Te@Au core-shell composites prepared in this study could be potentially exploited as efficient electrocatalysts.

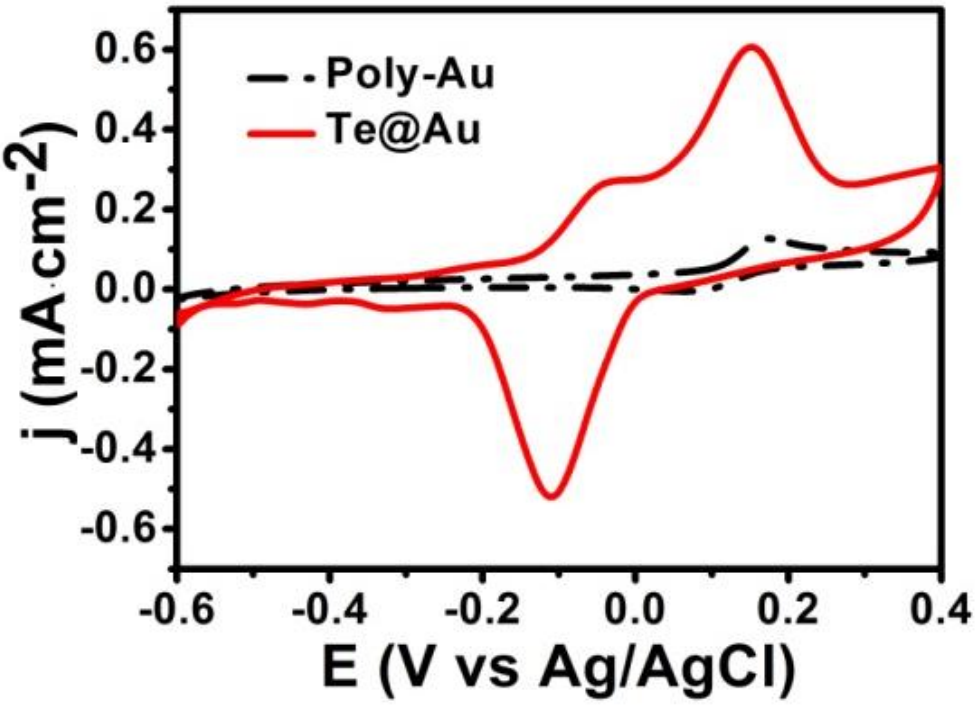


**Figure 6.** Cyclic voltammograms in 0.5 M KOH solution obtained with poly-Au and Te@Au electrodes.

Fig. 7 presents CVs of Te@Au hybrids and poly-Au electrodes conducted in a 0.5 M KOH solution containing 1.0 M isopropanol. The anodic peak potential at the Te@Au electrode is found to be around 360 mV, whereas the peak potential is 90 mV at the poly-Au electrodes. With the Te@Au electrode the anodic peak potential exhibits an approximate 200 mV positive shift, however, the current density is higher at corresponding potentials on Te@Au electrode than on poly-Au electrodes. Specifically, the peak current density is about 5 times for isopropanol oxidation on Te@Au electrode than that on poly-Au electrode, where the current density was calculated on the basis of ESA that was determined according to the method reported in literature. Although the anodic peak potential at the Te@Au electrode has shifted positively in relative to that at the bare Au electrode, the oxidation onset potential of the Te@Au electrode was at -0.40 V (vs Ag/AgCl electrode), which was more negative compared with that on poly-Au. The cathodic peak in Fig. 7 is significantly reduced when being compared with the CVs in Fig. 6, implicating that smaller amounts of Au oxides were produced during the forward scan in the isopropanol solution. The above results suggest that Au deposited on Te has a stronger catalytic effect on the electro-oxidation of isopropanol. Table 1 summarizes CV data from the electrocatalytic oxidation of isopropanol oxidation with various noble metals. It illustrates that the onset potential of our Te@Au catalysts is about the same as poly-Au, but is lower than other noble metal NPs hybrids. Overall, the catalytic performance of Te@Au is comparable to those Pt and Pd based catalysts. The fact that self-sacrificing approach consumes less amounts of Au in preparing the Te@Au hybrids makes the catalysts reported here a great advantage in future industrial applications.

**Table 1.** Electrochemical performance of different electrocatalysts in the isopropanol oxidation.

| Catalyst composition | Onset alcohol oxidation potential | $E_f$ (V) | Electrolyte | References |
|---|---|---|---|---|
| Pt–Ni/CCE | -0.2 | 0.45 (SCE) | 0.15M $C_3H_7OH$+0.1M $H_2SO_4$ | [41] |
| PdNPs–chitosan | -0.64 | 0.26 (Hg/HgO) | 0.73M $C_3H_7OH$+1.0M NaOH | [42] |
| Pt | 0.2 | 0.8 (RHE) | 1.0M $C_3H_7OH$+0.5M NaOH | [43] |
| Pd | 0.3 | 0.9 (RHE) | 1.0M $C_3H_7OH$+0.5M NaOH | [44] |
| PdAu4:1(4:1 by weight)/C | -0.67 | -0.4 (SCE) | 1.0M $C_3H_7OH$+0.5M KOH | [44] |
| Pt | -0.72 | -0.3 (SCE) | 1.0M $C_3H_7OH$+0.5M KOH | [45] |
| Pd | -0.78 | -0.39 (SCE) | 1.0M $C_3H_7OH$+0.5M KOH | [45] |
| Au | -0.46 | 0.08 (SCE) | 1.0M $C_3H_7OH$+0.5M KOH | [46] |
| Pt | -0.72 | -0.3 (SCE) | 1.0M $C_3H_7OH$+1.0M KOH | [47] |
| Pd | -0.78 | -0.39 (SCE) | 1.0M $C_3H_7OH$+1.0M KOH | [48] |
| Au | -0.4 | 0.07 (Ag/AgCl) | 1.0M $C_3H_7OH$+2.0M KOH | [48] |
| Pt | -0.8 | -0.4 (Ag/AgCl) | 1.0M $C_3H_7OH$+1.0M KOH | [48] |
| Au NP/C (1.0 nm) | 0.73 | 1.128 (RHE) | 1.0M $C_3H_7OH$+1.0MKOH | [49] |
| Au@Te | -0.40 | 0.36 (Ag/AgCl) | 1.0M $C_3H_7OH$+0.5M KOH | This work |

An anodic peak associated with isopropanol oxidation was also observed in the reverse sweeps. This oxidation peak was primarily associated with the removal of the adsorbed intermediate products that were formed during the forward scan. In literature[50, 51], the $I_f/I_b$ ratio, known as catalyst tolerance, which is extracted from the oxidative peaks current forward ($I_f$) and reversed ($I_b$) CV scans. with a higher ratio representing the better resistance against poisoning. Fig. 7 indicates that the Te@Au electrode was found to increase tolerance on poisoning. The improved tolerance of Te@Au hybrids catalysts on carbon intermediate products may be attributed to that reducible Au oxides promote the oxidation of intermediate products such as CO.

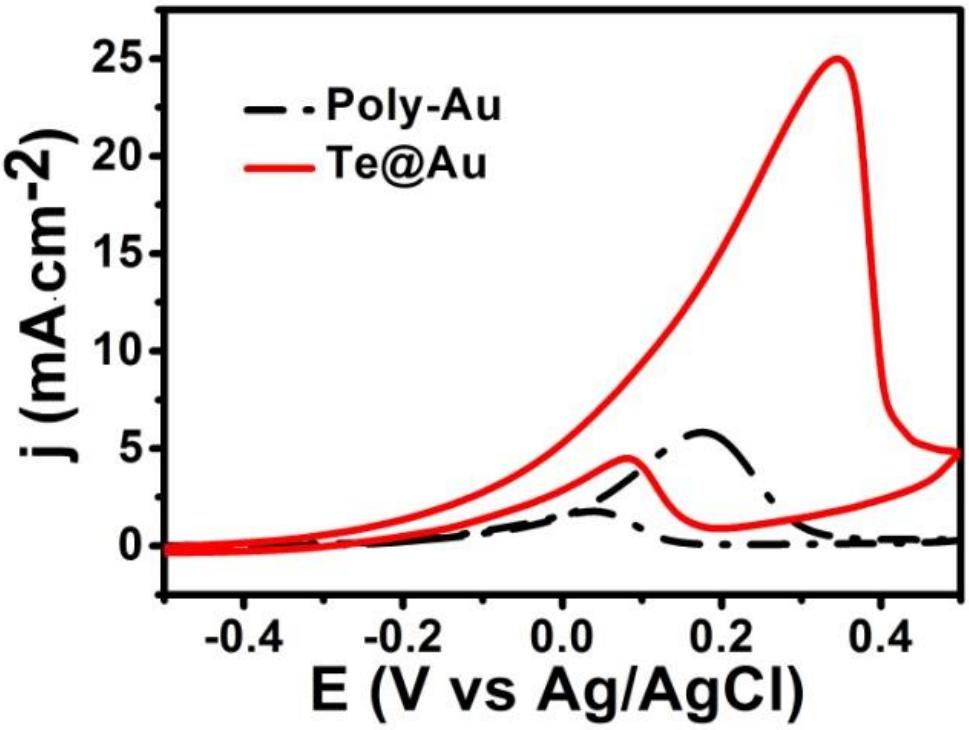


**Figure 7.** Cyclic voltammograms at poly-Au and Te@Au electrodes in a 0.5 M KOH solution containing 1.0 M isopropanol.

Fig. 8 shows the stability of isopropanal oxidation on the Te@Au and poly-Au catalysts in a 0.5 M KOH solution, measured at 0.2 V (versus Ag/AgCl). The Te@Au hybrids have a higher durability than the poly-Au. The decay of the oxidation current is very slower on Te@Au than that on poly-Au. After polarization for 2h, the current density is 0.98mA $cm^{-2}$, as opposed to the current that has decreased to 0.21 mA $cm^{-2}$ at the poly-Au electrode. The above observed current decay is generally associated with the poisoning by the oxidation products of isopropanol. Therefore, results in Fig. 8 provides further supports that Te@Au hybrids does not only enhance the catalytic activity of Au, but also leads to better durability toward poisoning[20,52].

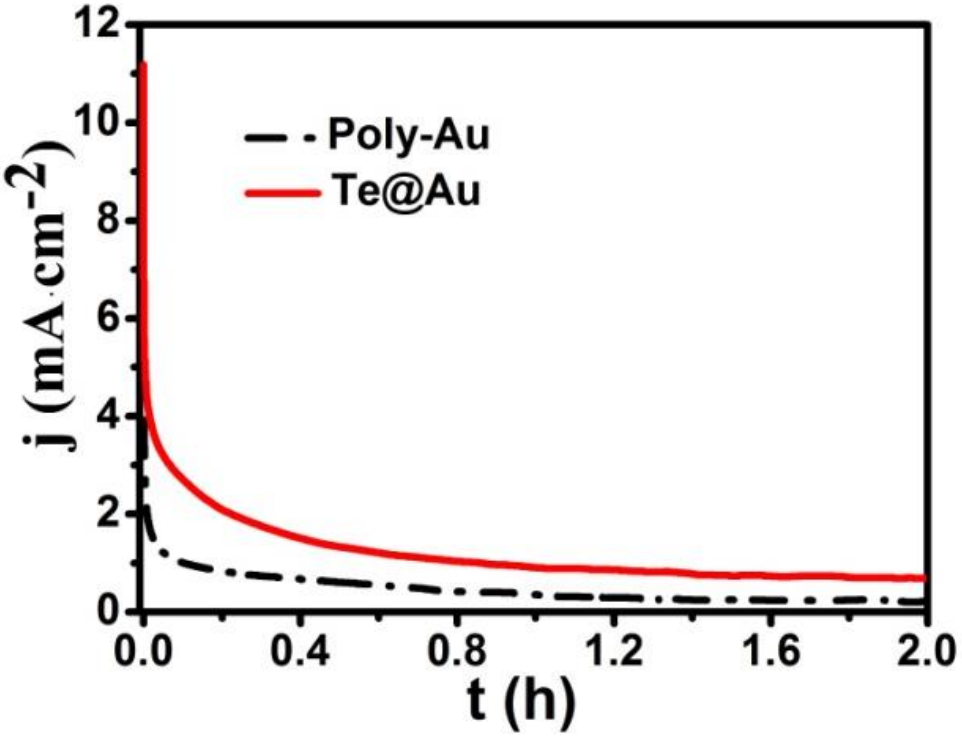


**Figure 8.** Chronoamperometric curves for the poly-Au and Te@Au electrodes in a 0.5 M KOH solution containing 1.0 M isopropanol. The applied potential was 0.2 V (vs Ag/AgCl electrode).

## 4. CONCLUSION

In summary, a novel hybrid of fusiform Te supported Au was synthesized via a simple two-phase interface reaction and subsequently template replacement process. Characterizations with SEM and TEM illustrate that the coating of Au film did not destroy the morphology of Te crystal. Using a Te core as the reducing agent ensured that the coated Au layer is very thin. Such an approach therefore reduced the need of precious metals such as Au. The higher catalytic performance of Te@Au toward isopropanol oxidation is most likely due to the combination of the synergistic effect between the Au precious metal and the Te semiconductor and the presence of numerous active sites on the surface and edge. The enhanced electrocatalytic activity and higher stability on fouling offers a new strategy for the design and construction of alcohol-based fuel cells.

ACKNOWLEDGMENTS
We are grateful for financial supports from National Natural Science Foundation of China (21471116, 21628102, 21601138, 21475097 and 51641210) and Zhejiang Provincial Natural Science Foundation of China (LZ15E020002, Y17E020012 and LZ17E020002).

## References

1. E. H. Yu, X. Wang, U. Krewer, L. Li, K. Scott, *Energy Environ. Sci.* 5 (2012) 5668.

2. Y. Xu and B. Zhang, *Chem. Soc. Rev*. 43 (2014) 2439.
3. F. Jaouen, E. Proietti, M. Lefèvre, R. Chenitz, J. P. Dodelet, G. Wu, H. T. Chung, C. M. Johnston, P. Zelenay, *Energy Environ. Sci.* 4 (2011) 114.
4. L. Zhang, Q. W. Chang, H. M. Chen, M. H. Shao, *Nano energy,* 29 (2016) 198.
5. M. Cao, D. Wu and R. Cao, *ChemCatChem* 6 (2014) 26.
6. Z. Qi, H. R. Geng, X. G Wang, C. C Zhao, H. Ji, C. Zhang, J. L. Xu and Z. H. Zhang, *J Power Sources*. 196 (2011) 5823.
7. H. Zhao, J.P. Dong, S.Y. Xing, Y. Li, J. Shen, J.Q. Xu, *J Hydrogen Energy*. 36 (2011) 9551.
8. J. Spendelow, A. Wieckowski, *Phys. Chem. Chem. Phys.*, 9 **(**2007) 2654.
9. Y. Liu, A. Ishihara, S. Mitsushima, N. Kamiya and K. Ota, *J. Electrochem. Soc*. 154 (2007) B664.
10. J. Moon, Y. Lee, S. Han, and K. Park, *Int J Hydrogen Energ* 39 (2015) 7798.
11. L. Li, L. Dou, H. Zhang, *Nanoscale* 6 (2014) 3753.
12. J. B. Xu, T. S. Zhao, Y. S. Li, W. W. Yang, *Int J Hydrogen Energ* 35 (2010), 9693.
13. G. Jeong, D. Choi, M. Kang, J. Shin, J. Kang, S. Kim, *RSC Adv*. 3 (2013) 8864.
14. Z. Yin, M. Chi, Q. Zhu, D. Ma, J. Sun, X. Bao, *J. Mater. Chem. A* 1 (2013) 9157.
15. H. J. Huang, X. Wang, *J. Mater. Chem. A*. 2 (2014) 6266.
16. G. Zhao, J. Huang, Z. Jiang, S. Zhang, L. Chen, Y. Lu, *Appl Catal B- Environ* 140-141 (2013) 249.
17. N. Li, Q. Zhou, S. Tian, H. Zhao, X. Li, J. Adkins, Z. Gu, L. Zhao, J. Zheng, *Electrochim Acta* 109 (2013) 546.
18. Z. Jin, Q. Wang, W. Zheng, X. Cui, *ACS Appl. Mater. Interfaces* 8 (2016) 5273.
19. J. Rodriguez, S. Ma, P. Liu, J. Hrbek, K. Evans and M. Perez, *Science* 318 (2007) 1757.
20. H. L. Jin, D. M Wang, Y. W. Zhao, H. Zhou, S Wang, J. C. Wang, *J. Power Sources* 215 (2012) 227.
21. O. H. Laguna, A. Perez, M. A. Centeno, J. A. Odriozola, *Appl. Catal. B-Environ*. 176-177 (2015) 385.
22. C. X Qi, S. D. Zhu, H. J. Su, H. Lin, R. G. Guan, *Appl. Catal. B -Environ.* 138-139 (2013) 104.
23. S. Li, H. Zhu, Z. F. Qin, G. F. Wang, Y. G. Zhang, Z. W. Wu, Z. K. Li, G. Chen, W. W. Dong, Z. G. Wu , L. R. Zheng, J. Zhang, T. D. Hu, J. G. Wang, *Appl. Catal. B-Environ.* 144 (2013) 498.
24. D. M. Alonso, S.G. Wettstein, J. A. Dumesic, *Chem. Soc. Rev.* 41 (2012) 8075.
25. S. Meenakshi, P. Sridhar, S. Pitchumani, *RSC Adv.* 4 (2014) 44386.
26. M. H. M. T. ssumpção, J. andenha, G. S. Buzzo, J. C. M. Silva, V. SpinacéE, A. O. Neto, Souza R. F. B. De, *J Power Sources* 253 (2014) 392.
27. S. Y. Shen, T. S. Zhao, J. B. Xu, Y. S. Li, *Energy Environ. Sci.* 4 (2011) 1428.
28. Y. B. Shen, A. F. Fan, D. Z. Wei, S. L. Gao, W. G. Liu, C. Han, B. Y. Cui, *RSC Adv.* 5 (2015) 29126.
29. H. An, L. N. Pan, H. Cui, D. D. Zhou, B. Wang, J. P. Zhai, Q. Li, Y. Pan, *J Electroanalytical Chem*. 741 (2015) 56.
30. V. K. Puthiyapura, D. J. L. Brett, A. E. Russell, W. F. Lin, C. Hardacre, *Chem. Commun.* 51(2015) 13412.
31. M. Christopher, C. M. Thompson, L. M. Carl, G. A. Somorjai Sum, *J. Phys. Chem. C.* 117 (2013) 26077.
32. Surbhi Sharma, Bruno G. Pollet, *J. Power Sources* 208 (2012) 96.
33. Y. W. Choi, I. Sinev, H. Mistry, I. Zegkinoglou, B. R. Cuenya, *ACS Catal.* 6 (2016) 3396.
34. A. S. Sharma, H. Kaur, D. Shah, *RSC Adv*. 6 (2016), 28688.
35. R. L. Oliveira, P. K. Kiyohara, L. M. Rossi, *Green Chem.* 12 (2010) 144.
36. Y. Maeda, T. Akita, M. Kohyama, *Catal Lett* 144 (2014) 2086.
37. D. Widmann, R. J. Beh, *Acc. Chem. Res.* 47 (2014) 740.
38. M. Yang, S. Li, Y. Wang, J. A. Herron, Y. Xu, L. F. Allard, S. Lee, J. Huang, M. Flytzani-Stephanopoulos, *Science*. 346 (2014) 1498.

39. M. Flytzani-Stephanopoulos, *Acc. Chem. Res.* 47 (2014) 783.
40. K. Yang, Y. F. Zhang, Y. Li, P. Huang, X. Chen, W. X. Dai, X. Z. Fu, *Appl. Catal. B-Environ.* 183 (2016) 206.
41. Biuck Habibi, Elaheh Dadashpour, *Electrochim Acta.* 88 (2013) 157.
42. M. Noroozifar, M. K. Motlagh, M.-S. Ekrami-Kakhki, R. Khaleghian-Moghadam, *J Appl Electrochem.* (2014) 44:233.
43. A. Santasalo-Aarnio, Y. Kwon , E. Ahlberg, K. Kontturi ,T. Kallio, M. T. M. Koper, *Electrochem Commun.*, 13 (2011) 466.
44. C. W. Xu, Z. Q. Tian, Z. C. Chen, S. P. Jiang, *Electrochem Commun.* 10 (2008) 246.
45. J. Q Ye, J. P. Liu, C. W. Xu, S. P. Jiang, Y. X. Tong, *Electrochem Commun.* 9 (2007) 2760.
46. M. Figueiredo, O. Sorsa, N. Doan, E. Pohjalainen, H. Hildebrand, P. Schmuki, B. P. Wilson, T. Kallio, *J Power Sources.* 275 (2015) 341.
47. J. P. Liu, J. Q. Ye, C. W. Xu, S. P. Jiang, Y. X. Tong, *J Power Sources.* 177 (2008) 67.
48. Y. Liu, Y. C. Zeng, R. Liu, H. B. Wu, G. L. Wang, D. X. Cao, *Electrochim Acta 7*6 (2012) 174.
49. Y. W. Choi, I. Sinev, H. Mistry, L. Zegkinoglou, B. R. Cuenya, *ACS Catal.*, 6 (2016), 3396
50. Z. W. Chen, L. L. Xu, W. Z. Li, M. Waje, Y. S. Yan, *Nanotechnology*. 17 (2006) 5254.
51. J. Zhang, H. Z. Yang, J. Y. Fang, S. Z. Zou, *Nano Lett.* 10 (2010) 638.
52. J. Liu, L. Cao, W. Huang, Z. Li, *ACS Appl. Mater. Interfaces* 3 (2011) 3552.